

Umbilical cord-derived mesenchymal stem cells exert anti-fibrotic action on hypertrophic scar-derived fibroblasts in co-culture by inhibiting the activation of the TGF β 1/Smad3 pathway

XIANGLONG MENG, XINXIN GAO, XINXIN CHEN and JIAAO YU

Department of Burns Surgery, The First Hospital of Jilin University, Changchun, Jilin 130000, P.R. China

Received January 30, 2019; Accepted August 23, 2019

DOI: 10.3892/etm.2021.9642

Abstract. A hypertrophic scar (HS) is a severe fibrotic skin disease that causes disfigurement and deformity. It occurs after deep cutaneous injury and presents a major clinical challenge. The present study aimed to evaluate the effects of umbilical cord-derived mesenchymal stem cells (UCMSCs) on hypertrophic scar fibroblasts (HSFs), one of the main effector cells for HS formation, in a co-culture system and to investigate the potential underlying molecular mechanism. Cultured HSFs were divided into control and co-culture groups. The proliferation ability of HSFs was evaluated using cell counting kit-8 and the percentage of Ki67-positive fibroblasts was assessed by immunofluorescence. The apoptosis of HSFs was determined using a TUNEL assay and by assessing the expression of caspase-3 via western blotting. A scratch wound healing assay was employed to examine the migration of HSFs. The expression levels of HS-associated genes (collagen type Ia 2 chain, collagen type III α 1 chain and actin α 2 smooth muscle) and proteins (collagen I, collagen III and α -smooth muscle actin) were measured by reverse transcription-quantitative PCR (RT-qPCR) and western blotting, respectively, to assess the pro-fibrotic phenotype of HSFs. The modulation of the transforming growth factor β 1 (TGF β 1)/Smad3 pathway in HSFs was evaluated by measuring the protein levels of TGF β 1, Smad3 and phosphorylated Smad3 using western blotting, and the mRNA levels of *TGF β 1* and several other target genes (cellular communication network factor 2, metalloproteinase inhibitor 1 and periostin) were measured by RT-qPCR. The proliferative and migratory ability of co-cultured HSFs was suppressed compared with controls, and no significant difference in apoptosis was observed between the two groups. The pro-fibrotic phenotype of co-cultured HSFs was inhibited due to a decline in expression levels of HS-associated genes and proteins.

Furthermore, co-culture with UCMSCs inhibited the activation of the TGF β 1/Smad3 pathway. In conclusion, the present study indicated that UCMSCs may exert an anti-fibrotic action on HSFs in co-culture through inhibition of the TGF β 1/Smad3 pathway, which suggests a potential use for UCMSCs in HS therapy.

Introduction

A hypertrophic scar (HS) is a severe fibrotic cutaneous disorder characterized by morphological abnormality and limited movement (1). It often occurs after deep skin injuries such as extensive burns. The incidence of HSs during cicatrix formation after a burn injury is up to 70% (2). This not only damages the physical and psychological health of patients, but also places a heavy economic burden on their families and society. Development of an effective therapy for HSs would be highly beneficial.

The development of a curative strategy for hypertrophic scarring relies on investigation into the underlying pathophysiological mechanism (3). Previous studies of HSs have revealed that their formation is driven by an abnormal composition and excessive deposition of extracellular matrix (ECM), and that overactive hypertrophic scar fibroblasts (HSFs) are one of the main effector cells responsible for these pathological changes (4). Furthermore, the transforming growth factor β 1 (TGF β 1)/Smad3 pathway has been recognized as a principal cellular signaling pathway in the promotion of fibrosis of HSFs (5). The phosphorylation of Smad3 is an important step in this signaling cascade (6,7). Regulation of this pathway in HSFs may have an essential role in future HS therapies (3).

Application of mesenchymal stem cells (MSCs) in HS therapy is a possible approach to treatment (8,9). MSCs derived from different tissues have different biological characteristics, but research has largely been focused on bone marrow-derived MSCs (BM-MSCs) and adipose-derived MSCs (AD-MSCs) (10-13). There are few reports focusing on the therapeutic benefit of umbilical cord-derived MSCs (UCMSCs), which possess a high proliferative ability, weak immunogenicity and a specific anti-fibrotic paracrine profile (14-16). To the best of our knowledge, there has been limited research into the exact mechanism of administration of UCMSCs for HS therapy.

In the present study the effect of UCMSCs on the pro-fibrotic phenotype of HSFs in a co-culture system and

Correspondence to: Dr Jiaao Yu, Department of Burns Surgery, The First Hospital of Jilin University, 1409 Ximinzhong Street, Changchun, Jilin 130000, P.R. China
E-mail: egfg74@163.com

Key words: hypertrophic scar fibroblasts, umbilical cord derived mesenchymal stem cells, transforming growth factor β 1, Smad3, co-culture

the potential molecular mechanisms underlying this regulation were investigated. Pro-fibrotic phenotype was measured through assessment of fibrosis-related cellular behaviours, including cell proliferation, apoptosis, migration and the expression of HS-associated genes and proteins.

Materials and methods

Isolation and culture of cells. UCMSCs were kindly provided by Stem Cell Bank, Chinese Academy of Sciences and were cultured in DMEM containing 10% fetal bovine serum (FBS) and antibiotics (penicillin, 100 U/ml; streptomycin, 0.1 mg/ml) at 37°C with 5% CO₂. These UCMSCs possess the ability to differentiate into adipose tissue, bone and cartilage and are CD29, CD44, CD73, CD90, CD105 and CD166 positive, while CD14, CD31, CD34, and CD45 negative.

Primary HSFs were cultured from the tissues of six patients (3 male and 3 female; age, 17 months to 27 years) with HSs who had received a cicatrixectomy in the Department of Burn Surgery of The First Hospital of Jilin University (Changchun, China) from April 2016 to July 2017. Briefly, HS tissue mass was washed twice with phosphate-buffered saline and cut into ~1-mm³ sections under sterile conditions. Washed sections were placed in a culture plate with a distance of 1 cm between each other at 37°C for 30 min, and then incubated in DMEM containing 10% FBS and antibiotics (penicillin, 100 U/ml; streptomycin, 0.1 mg/ml) at 37°C with 5% CO₂. All cell culture reagents were supplied by Gibco; Thermo Fisher Scientific, Inc. When UCMSCs and HSFs reached 90% confluence, they were trypsinized and prepared for subculture. UCMSCs at passages 6-8 and HSFs at passages 2-4 were used in the experiments described below.

Co-culture of cells. Transwell culture plates (Millicell®; EMD Millipore) were used to develop the co-culture system [a 96-well culture plate was used for the Cell Counting Kit-8 (CCK-8) assay, and six-well culture plates were used for the other experiments in this study]. UCMSCs at passages 6-8 were harvested and then seeded on the upper chamber of a transwell culture plate at a density of 1x10⁴ cells/cm². HSFs at passages 2-4 were harvested and seeded on the lower chamber at the same density. The co-culture system was cultured in DMEM containing 10% FBS and antibiotics (penicillin, 100 U/ml; streptomycin, 0.1 mg/ml). The cultured HSFs were divided into co-culture and control groups based on the culture conditions. No UCMSCs were included in the upper chamber of the control group. Cells were co-cultured for 12-72 h for proliferation analysis, 48 h for apoptosis analysis, and for 72 h for migration analysis and detecting gene and protein expression levels.

CCK-8 assay. CCK-8 (Beijing Solarbio Science & Technology Co., Ltd.) was used to monitor cell proliferation. Briefly, HSFs were seeded at 5x10³ cells per well in a 96-well culture plate with three replicates per sample. At 12, 24, 36, 48 and 72 h after cell attachment, 10 μl of CCK-8 solution was added to each well. After incubation for 1 h, the absorbance was measured at 450 nm using a microplate reader (Thermo Fisher Scientific, Inc.).

Immunofluorescence. The media of prepared HSFs were discarded, and pre-cooled methanol was added to fix the cells for 30 min at room temperature. Cells were incubated with PBS containing 0.2% Triton X-100 for 15 min at room temperature for permeabilization, and with TBST (0.5% Tween-20) containing 1% BSA for 30 min at room temperature for blocking. For Ki67 staining, the cells were incubated with a primary anti-Ki67 antibody (1:100; cat. no. ab197234; Abcam) at 4°C overnight followed by incubation with the corresponding CY3-conjugated secondary antibody (1:2,000; cat. no. ab6939; Abcam) at 37°C for 2 h. For TUNEL staining, the cells were incubated with a TUNEL reagent (Beyotime Institute of Biotechnology) at 37°C for 1 h. Finally, after the nuclei were counterstained with DAPI (1:1,000; Beyotime Institute of Biotechnology) for 10 min at room temperature, the slides were mounted with Antifade Mounting Medium (Beyotime Institute of Biotechnology). Images of each slide were captured at three random fields of view using an inverted fluorescence microscope (magnification, x100; IX73; Olympus Corporation). Total nuclei (blue) and Ki67 or TUNEL-positive (red) cells were quantified using ImageJ software (version 1.51w; National Institutes of Health).

Scratch wound closure assay. Cell migration was tested using a scratch wound closure assay. In brief, HSFs of co-culture and control groups were cultured in a six-well culture plate at a density of 1x10⁴ cells/cm² with DMEM containing 10% FBS until the cell confluence reached 100%. A 1-ml pipette tip was used to make a scratch wound in the middle of each well. After washing three times with PBS, the medium was changed to serum-free DMEM for 72 h. Images were acquired using an inverted microscope (magnification, x40; Olympus Corporation) after 24, 48 and 72 h. Wound area was measured using ImageJ software (version 1.51; National Institutes of Health). Results are shown as the percentage of area closed, which was calculated through normalizing the wound space of each time point to that of 0 h. Images of each well were captured at three random fields of view.

Reverse transcription-quantitative PCR (RT-qPCR). Total RNA was isolated, and RT was performed as previously described (17). Briefly, total RNA was isolated from HSFs from the control group and the group co-cultured with UCMSCs for 3 days using TRIzol® reagent (Invitrogen; Thermo Fisher Scientific, Inc.). cDNA was synthesized using the TransScript All-in-One First-Strand cDNA Synthesis SuperMix (Beijing Transgen Biotech Co., Ltd.). FastStart Universal SYBR Green Master (ROX) (Roche Diagnostics GmbH) was used for qPCR using a Stratagene Mx3005P instrument (Agilent Technologies, GmbH). The reaction conditions were: Initial denaturation at 95°C for 10 min; 40 cycles of denaturation at 95°C for 30 sec and annealing at 60°C for 1 min; dissociation at 95°C for 1 min, annealing at 55°C for 30 sec, and final extension at 95°C for 30 sec. The primers used in this study for gene amplification are listed in Table I. Expression levels of target genes were normalized to that of *GAPDH* and the 2^{-ΔΔC_q} method was used to calculate the relative expression levels of genes (18). Each sample was run in triplicate wells.

Western blotting. HSFs of co-culture and control groups were harvested and washed with PBS. The cells were processed

Table I. Sequences of primers used for PCR.

Gene	Primer sequence (5'→3')	
	Forward	Reverse
<i>COL1A2</i>	GAGGGCAACAGCAGGTTCACTTA	TCAGCACCACCGATGTCCA
<i>COL3A1</i>	CCACGGAAACACTGGTGGAC	GCCAGCTGCACATCAAGGAC
<i>ACTA2</i>	GACAATGGCTCTGGGCTCTGTAA	TGTGCTTCGTCACCCACGTA
<i>TGFβ1</i>	AACTCCGGTGACATCAAAAAGATAA	TGCTGAGGCTCAAGTTAAAAGT
<i>CTGF</i>	CTGGAAGGACTCTCCGCTGCGG	GCGACCCGCACAAGGGCCTAT
<i>TIMP1</i>	ACCCACAGACGGCCTTCTGCAATT	AACGCTGGTATAAGGTGGTCTGGTT
<i>POSTN</i>	CTCAGAGCAGATGCCAAGCCTAATTG	GTGTGATCCATTTGATTGATCAGGTCCT
<i>GAPDH</i>	GCACCGTCAAGCTGAGAAC	TGGTGAAGACGCCAGTGGA

COL1A2, collagen type I α 2 chain; COL3A1, collagen type III α 1 chain; ACTA2, actin α 2 smooth muscle; TGF β 1, transforming growth factor β 1; CTGF, cellular communication network factor 2; TIMP1, metalloproteinase inhibitor 1; POSTN, periostin.

with RIPA lysis buffer (CST Biological Reagents Co., Ltd.) supplemented with phenylmethylsulphonyl fluoride (Thermo Fisher Scientific, Inc.), protease inhibitor cocktail (TransGen Biotech Co., Ltd.) and phosphatase inhibitor cocktail (TransGen Biotech Co., Ltd.). Protein concentration was determined using a bicinchoninic acid (BCA) protein assay kit (Beyotime Institute of Biotechnology). Western blotting was performed as previously described (17). In brief, 30 μ g of protein from each sample was separated in 8% (for collagen I and III), 10% [for TGF β 1, α -smooth muscle actin (α -SMA), Smad3 and phosphorylated (p)-Smad3] or 12% (for caspase-3) SDS-PAGE gels, and then electro-transferred to PVDF membranes (Immobilon-P, EMD Millipore) for immunoblotting analysis. After blocking with 5% bovine serum albumin (Sigma-Aldrich; Merck KGaA) in TBST (0.5% Tween-20) for 1 h at room temperature, the primary antibodies anti-collagen I (1:1,000; cat. no. 14695-1-AP; ProteinTech Group, Inc.), anti-collagen III (1:500; cat. no. 22734-1-AP; ProteinTech Group, Inc.), anti- α -SMA (1:1,000; cat. no. ab32575; Abcam), anti- β -actin (1:2,000; cat. no. 60008-1-Ig; ProteinTech, Group Inc.), anti-TGF β 1 (1:1,000; cat. no. 21898-1-AP; ProteinTech Group, Inc.), anti-Smad3 (1:1,000; cat. no. ab40854; Abcam), anti-p-Smad3 (1:500; cat. no. ab52903; Abcam) and anti-caspase-3 (1:500; cat. no. ab13847; Abcam) were incubated with the PVDF membranes at 4°C overnight. Following incubation with the appropriate horseradish peroxidase-conjugated secondary antibodies (1:5,000; goat anti-mouse cat. no. SA00001-1; goat anti-rabbit cat. no. SA00001-2; ProteinTech Group, Inc.) for 1 h at room temperature, proteins were detected by chemiluminescence using the EasySee Western Blot kit (TransGen Biotech Co., Ltd) in a myECL™ imager (Thermo Fisher Scientific, Inc.), and the band intensities were quantified using ImageJ software.

Statistical analysis. The quantified data are presented as the mean \pm SD for the CCK-8 assay, immunofluorescence (percentage of Ki67- or TUNEL-positive cells), RT-qPCR and scratch wound closure assay, and as the mean \pm SEM for western blotting. The differences between the two groups were analysed by Student's t-test using GraphPad Prism (version

7.00; Graph Pad Software Inc.) statistical package. A value of $P < 0.05$ was considered to indicate a statistically significant difference. All experiments were repeated at least three times.

Results

UCMSCs suppress the proliferation of HSFs in co-culture. In order to determine whether UCMSCs affect the proliferation of HSFs in a co-culture system, the cell viability of HSFs cultured with or without UCMSCs at different time points was assessed using a CCK-8 assay and the percentage of Ki67-positive fibroblasts determined through immunofluorescence. After co-culture with UCMSCs for 24, 36, 48, and 72 h, the cell viability of HSFs was significantly lower compared with their respective control groups (24 h, $P < 0.05$; 36, 48 and 72 h, $P < 0.01$; Fig. 1A). Additionally, the percentages of Ki67-positive fibroblasts in the co-culture group were significantly lower than that in the control group after culturing for 48 h ($P < 0.001$, Fig. 1B and C). These differences suggested that UCMSCs could suppress the proliferative ability of HSFs in co-culture.

UCMSCs do not influence the apoptosis of HSFs in co-culture. The apoptosis of HSFs was measured via a TUNEL assay and by assessing the expression of caspase-3, a key apoptosis-related protein, through western blotting after 48 h of co-culture. As shown in Fig. 2A and B, the TUNEL assay revealed that there was no significant difference between the percentage of apoptosis-positive cells from the two groups. Moreover, the protein levels of cleaved caspase-3, which indicated the apoptosis level, revealed that there was no significant difference between levels in the HSFs of co-cultured groups compared with those in the controls (Fig. 2C and D). Taken together, the results demonstrated that UCMSCs had no influence on the rate of apoptosis of HSFs in a co-culture system.

UCMSCs inhibit the migration of co-cultured HSFs. To study the effect of UCMSCs on the migration of HSFs in co-culture, a scratch wound healing assay was performed. Representative images of this assay at the time points 24, 48 and 72 h after

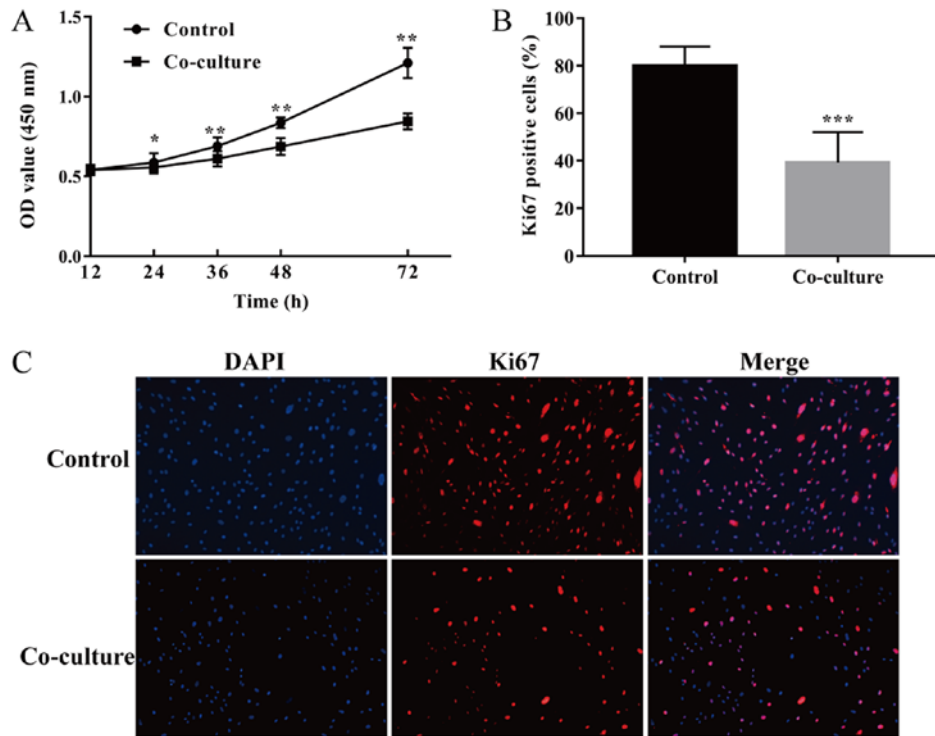


Figure 1. Effect of UCMSCs on the proliferation of HSFs in a co-culture system. (A) Cell proliferation was measured using a cell counting kit-8 assay at the time points 12, 24, 36, 48 and 72 h. * $P < 0.05$ and ** $P < 0.01$ vs. the co-culture group. (B) The percentage of Ki67-positive HSFs (red) was detected by (C) immunofluorescence after co-culture for 48 h. Original magnification, $\times 100$. Data are presented as the mean \pm SD. *** $P < 0.001$ vs. the control group. HSF, hypertrophic scar fibroblast; UCMSC, umbilical cord-derived mesenchymal stem cell.

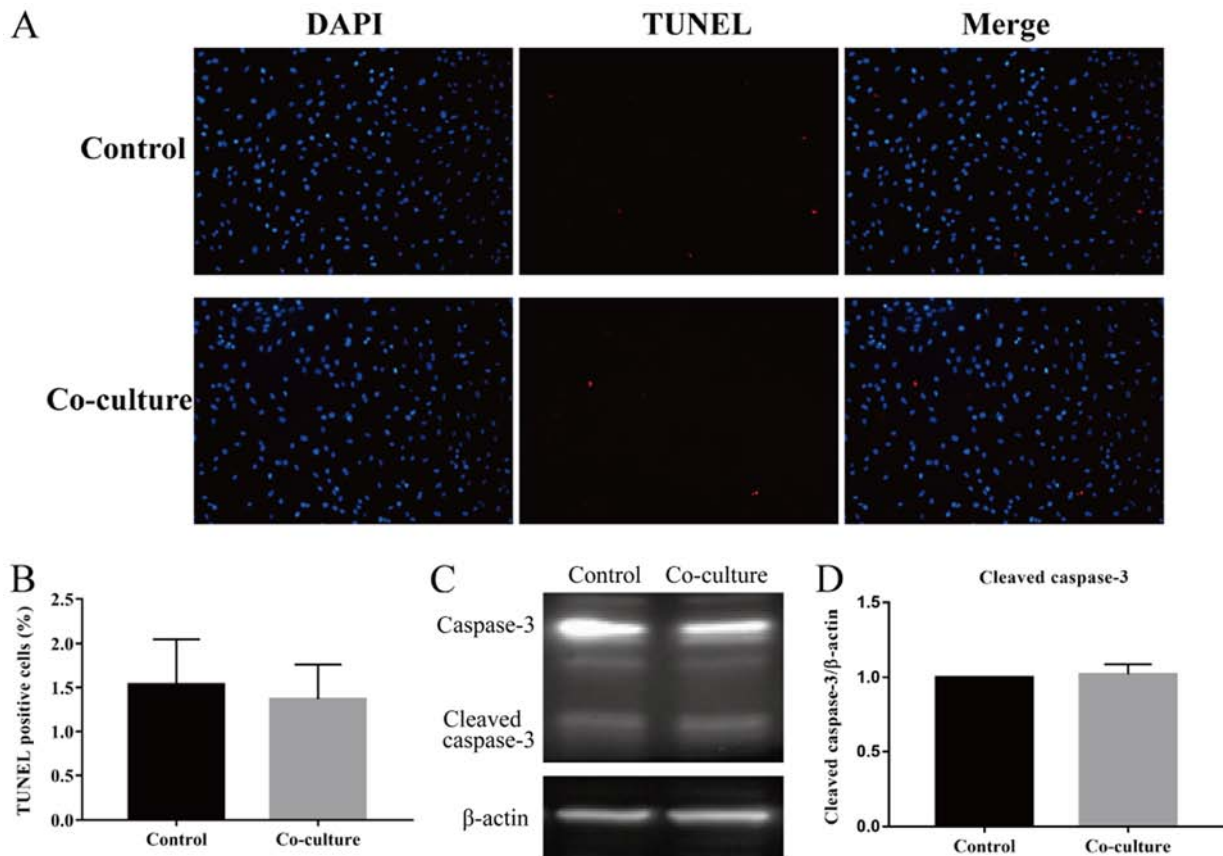


Figure 2. Effect of UCMSCs on the apoptosis of HSFs in a co-culture system. (A) Immunofluorescence was used to detect (B) the percentage of TUNEL-positive HSFs (red) after co-culture for 48 h. Original magnification, $\times 100$. Data are presented as the mean \pm SD. (C) The levels of caspase-3 and cleaved caspase-3 were assessed by western blotting and (D) the levels of cleaved caspase-3 were quantified. Data are presented as the mean \pm SEM. HSF, hypertrophic scar fibroblast; UCMSC, umbilical cord-derived mesenchymal stem cell.

scratching showed that the migration ability of co-cultured HSFs into the scratched space was inhibited compared with that of controls (Fig. 3A). The scratch wound of the controls cultured without UCMSCs was almost closed after 72 h; however, the corresponding co-cultured subset was not. The percentage of wound closure area at different time points compared with the 0 h controls was quantified. As shown in Fig. 3B, after 24, 48 and 72 h of culture, respectively, 40.23±1.73, 70.4±1.8 and 86.52±1.1% of the scratched space was filled by the migrated HSFs in the control groups; by contrast, 28.69±1.85, 36.64±0.9 and 47.19±1.36% of space was filled by the migrated HSFs in the co-culture groups, indicating a significant difference between the two groups in terms of HSF migration (24, 48 and 72 h, $P<0.01$; Fig. 3B). These data demonstrated that UCMSCs could significantly inhibit the migration ability of HSFs in co-culture.

UCMSCs reduce HS-associated gene and protein expression in HSFs in co-culture. The expression of HS-associated genes and proteins was measured to examine the effect of UCMSCs on the pro-fibrotic phenotype of HSFs in a co-culture system. The mRNA levels of collagen type I α 2 chain (*COL1A2*), collagen type III α 1 chain (*COL3A1*) and actin α 2 smooth muscle (*ACTA2*), and the protein levels of collagen I, collagen III and α -SMA, which play essential roles in HS formation, were assessed by RT-qPCR and western blotting, respectively (Fig. 4). RT-qPCR showed that the mRNA levels of *COL1A2*, *COL3A1* and *ACTA2* of HSFs from the co-culture groups were significantly lower than those from their respective control groups (all, $P<0.01$; Fig. 4A-C). Consistent with the changes in the mRNA levels, the protein levels of collagen I, collagen III and α -SMA in the co-cultured HSFs decreased compared with the controls, as shown through western blotting (Fig. 4D) and further quantitative and statistical analysis (collagen I, $P<0.05$, Fig. 4E; collagen III and α -SMA, $P<0.01$, Fig. 4F and G). All the above results suggested that UCMSCs could inhibit the pro-fibrotic phenotype of HSFs in co-culture.

TGF β 1/Smad3 signaling pathway was inhibited in HSFs co-cultured with UCMSCs. To further investigate the potential mechanism underlying the anti-fibrotic effect of UCMSCs, levels of the related key protein molecules of the TGF β 1/Smad3 pathway in HSFs were assessed. As shown in Fig. 5A, the levels of TGF β 1 and p-Smad3 in HSFs co-cultured with UCMSCs were significantly reduced (TGF β 1, $P<0.05$, Fig. 5B; p-Smad3, $P<0.01$, Fig. 5D), whereas no significant difference between the levels of total Smad3 (t-Smad3) protein was observed (Fig. 5C). However, the ratio of p-Smad3 to t-Smad3 was significantly decreased in co-culture group compared with the control ($P<0.01$, Fig. 5E). The mRNA levels of *TGF β 1* and other important genes targeted by this pathway [cellular communication network factor 2 (*CTGF*), metalloproteinase inhibitor 1 (*TIMPI*) and periostin (*POSTN*)] were then examined. Statistical analysis indicated that the transcription of these genes in HSFs from the co-cultured group was inhibited compared with the control (*TGF β 1*, $P<0.01$, Fig. 5F; *CTGF*, $P<0.01$, Fig. 5G; *TIMPI*, $P<0.05$, Fig. 5H; *POSTN*, $P<0.0001$, Fig. 5I). This suggested that UCMSCs may inhibit the fibrosis of HSFs by inhibiting the TGF β 1/Smad3 pathway, and that the reduction of TGF β 1 and inhibited phosphorylation of Smad3 played key roles in this regulation.

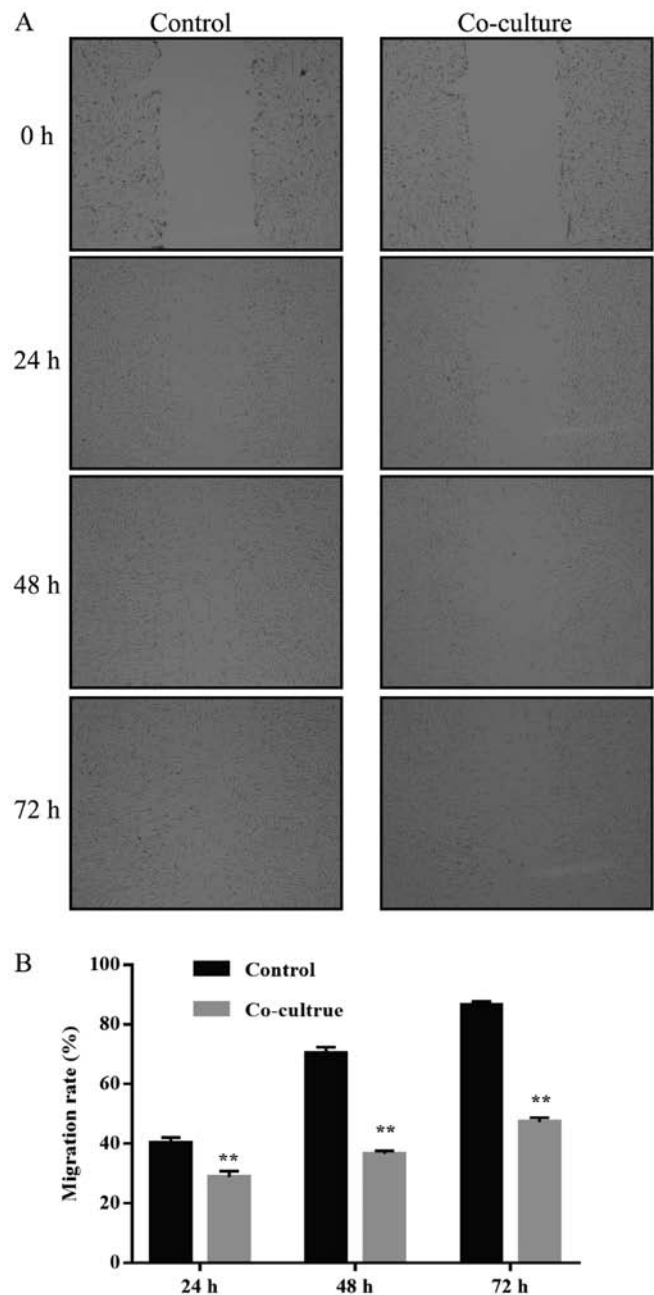


Figure 3. Effect of UCMSCs on the migration of HSFs in a co-culture system. The scratch wound healing assay was employed to measure the migration of HSFs *in vitro*. (A) Cell migration immediately after a scratch and at 24, 48 and 72 h after scratching. Original magnification, x40. (B) Quantitative analysis of cell migration at 24, 48 and 72 h after scratching. Data are presented as the mean \pm SD. ** $P<0.01$ vs. the control group. HSF, hypertrophic scar fibroblast; UCMSC, umbilical cord-derived mesenchymal stem cell.

Discussion

Due to improvements in acute burn care, in recent decades mortality due to extensive deep burns has significantly decreased (19). In recent years, HSFs, which can cause severe physical and psychological problems in patients who survive massive burns, have become the greatest unmet challenge in burn care (1). In order to address this problem a variety of treatments has been developed, including surgical approaches, compressive dressing, laser therapy and local drug injection (20). Existing studies and trials have shown that though

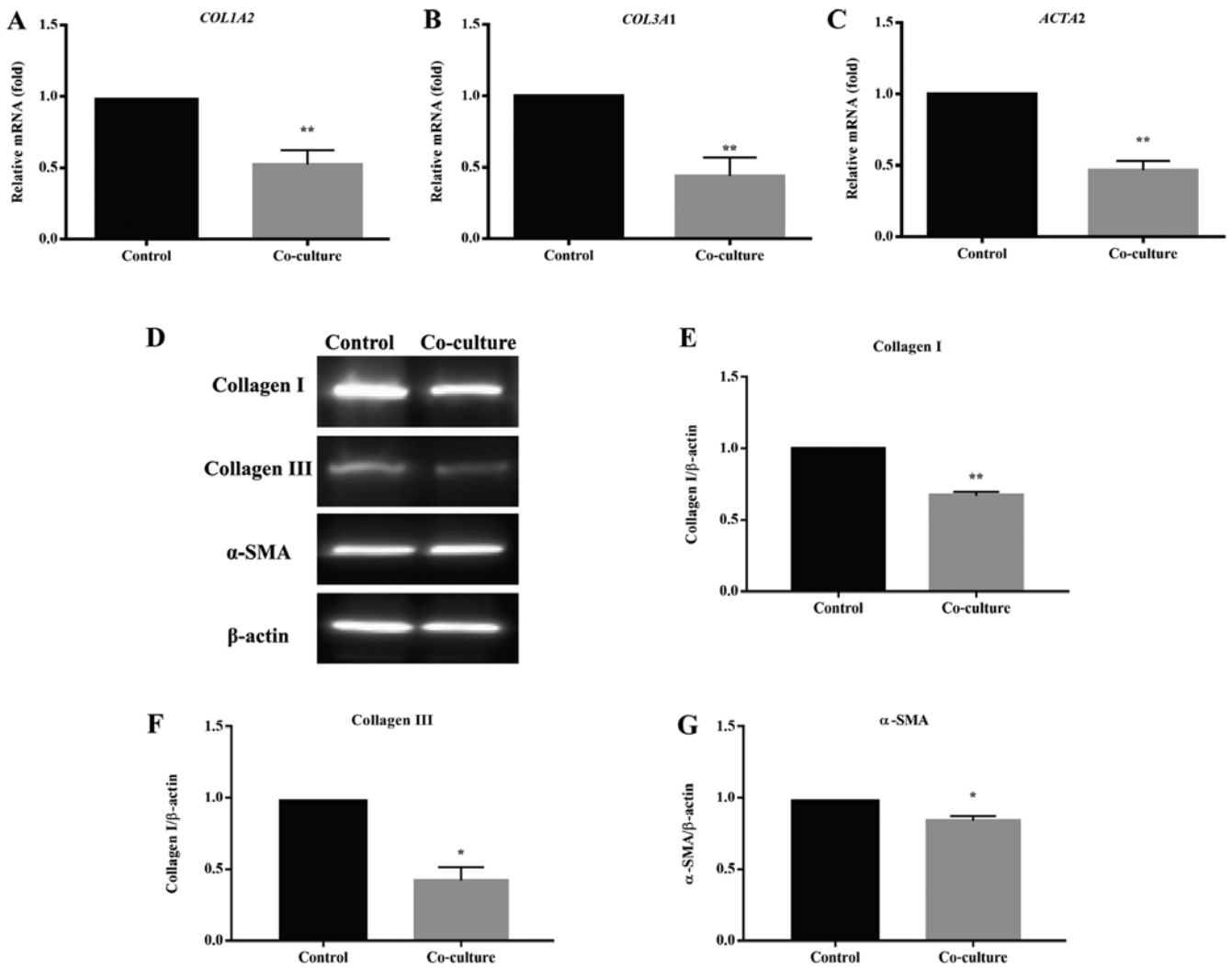


Figure 4. Effect of UCMSCs on HS-associated gene and protein expression of HSFs in a co-culture system. The relative mRNA levels of (A) *COL1A2*, (B) *COL3A1* and (C) *ACTA2* were detected by reverse transcription-quantitative PCR. Data are presented as the mean \pm SD. (D) Western blotting was used to determine the protein levels of (E) collagen I, (F) collagen III and (G) α -SMA. Data are presented as the mean \pm SEM. * P <0.05 and ** P <0.01 vs. the control group. α -SMA, α -smooth muscle actin; ACTA2, actin α 2 smooth muscle; COL1A2, collagen type I α 2 chain; COL3A1, collagen type III α 1 chain; HS, hypertrophic scar; HSF, hypertrophic scar fibroblast; UCMSC, umbilical cord-derived mesenchymal stem cell.

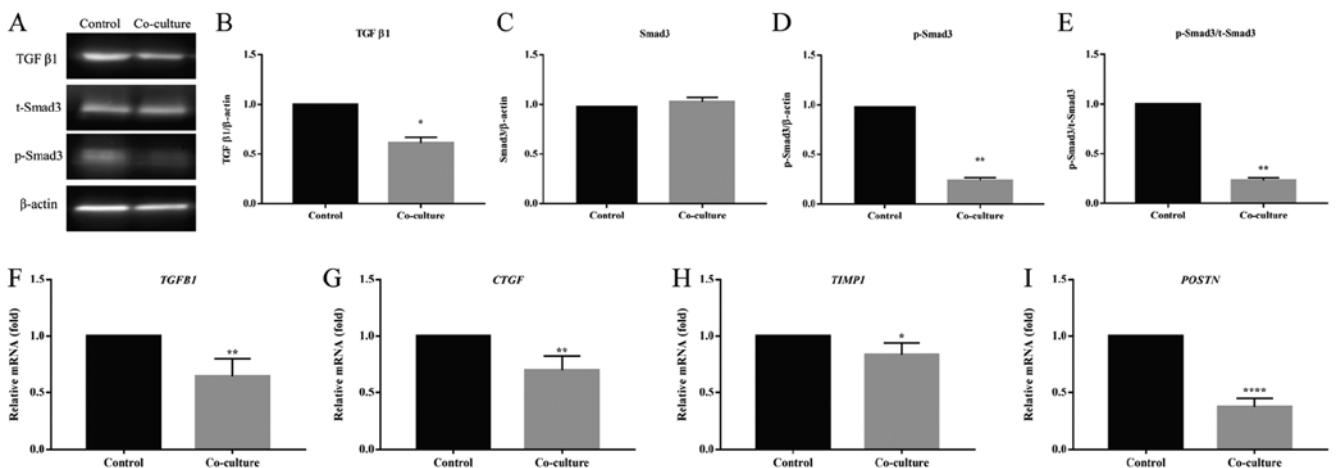


Figure 5. Effect of UCMSCs on the activation of the TGF β 1/Smad3 pathway of HSFs in a co-culture system. (A) Western blotting was used to determine the protein levels of (B) TGF β 1, (C) t-Smad3 and (D) p-Smad3, and (E) the ratio of p-Smad3 to t-Smad3. Data are presented as the mean \pm SEM. The relative mRNA levels of (F) *TGFBI*, (G) *CTGF*, (H) *TIMP1* and (I) *POSTN* were detected by reverse transcription-quantitative PCR. Data are presented as the mean \pm SD. * P <0.05, ** P <0.01 and **** P <0.0001 vs. the control group. CTGF, cellular communication network factor 2; HSF, hypertrophic scar fibroblasts; p, phosphorylated; t, total; TGFBI, transforming growth factor β 1; TIMP1, metalloproteinase inhibitor 1; POSTN, periostin; UCMSC, umbilical cord-derived mesenchymal stem cells.

these methods are effective in addressing HSs, they have limitations and can be accompanied by severe side-effects (3,20). The development of a comprehensive treatment for this disease remains a long and arduous task.

MSC therapy in wound healing has been widely studied (21). Previous studies have demonstrated that MSCs attenuate scarring through their involvement in all overlapping scar formation phases: inflammation, proliferation and remodeling (22). Liu *et al* (23) reported that BM-MSCs repressed HS formation through inflammatory regulation in a rabbit model. Domergue *et al* (24) proposed that, in a nude mouse model, injection of AD-MSCs produced an anti-fibrotic effect during the remodeling phase of HS formation. However, Ding *et al* (25) found that the fibrosis of deep dermal fibroblasts was reinforced by BM-MSCs in a co-culture model. These studies illustrate the regulatory effect of MSCs on scar formation, and indicate that MSCs could activate normal dermal fibroblasts and inhibit HS fibroblasts (3). Among the literature on MSCs as a therapy for HSs, there are few reports focusing on UCMSCs. However, there is increasing evidence to suggest that UCMSCs may inhibit fibrosis in other fibrotic diseases (26-28). UCMSCs are characterized by their high proliferation rate, weak immunogenicity, non-invasive acquisition and special paracrine factors (14-16). When compared with other tissue-sourced MSCs, the paracrine profile of UCMSCs contains a higher level of hepatocyte growth factor (HGF) (29), which is defined as an anti-fibrotic factor, and lower levels of vascular endothelial growth factor and epidermal growth factor (16), which have been demonstrated to promote the progression of fibrosis. These findings support the hypothesis that UCMSCs are a promising target for treatment against HS formation. Consistent with this hypothesis, the present study demonstrated that UCMSCs could inhibit proliferation and migration, as well as the expression of HS-related genes in HSFs in a co-culture system. UCMSCs had no effect on the apoptosis of HSFs. These results suggest that UCMSCs may be beneficial as a clinical treatment against HS formation. Further research is required to confirm this and will be focused on the *in vivo* experiments and the clinical application of UCMSCs.

Investigation into the mechanism underlying the anti-fibrotic function of UCMSCs suggested that UCMSCs could regulate the TGF β 1/Smad3 pathway of HSFs *in vitro*, through inhibition of TGF β 1 expression and the phosphorylation of Smad3. TGF β 1 plays a fundamental role in HS formation, and Smad3 acts as a convergent node in the pathway downstream of TGF β 1 receptors. Smad3 forms a complex with Smad2 and Smad4 and functions as a transcription factor that induces aberrant ECM deposition and hyperactivity of fibroblasts (5-7). Additionally, Smad2 has been reported to be involved in the regulation of the differentiation of myofibroblasts mediated by UCMSC-derived exosomal microRNAs (30). The mechanisms underlying the anti-fibrotic effect of UCMSCs on HSFs must be further elucidated in order to develop treatment against HSs.

In previous studies, MSC conditioned medium and the isolated exosomes of MSCs have been used to stimulate target cells in order to test the effects of MSCs *in vitro* (31,32). The present study adopted a transwell co-culture system to investigate the interaction between UCMSCs and HSFs. *In vivo*, target cells are not only unilaterally subject to the effect of MSCs, but they can also simultaneously influence the paracrine release of MSCs via interaction in the unique

microenvironment (33). A co-culture system provided a better *in vitro* simulation for cell-cell interaction compared with the administration of conditioned medium or isolated exomes (34,35). However, there are still numerous problems worth studying to explore this complex interaction, such as the mechanism of direct cell-cell interaction and interaction in a 3D co-culture system (36).

In conclusion, the present study indicates that UCMSCs may play a valuable role in HS therapy by exerting an anti-fibrotic action on HSFs, inhibiting their proliferation and migration, and reducing the expression of HS-associated genes and proteins. Suppression of the TGF β 1/Smad3 pathway appears to be a part of the molecular mechanism underlying this regulation.

Acknowledgements

Not applicable.

Funding

The current study was supported by the Natural Science Foundation of Jilin Provincial Science and Technology Department Project (grant no. 20160101141JC).

Availability of data and materials

The datasets used and/or analyzed during the current study are available from the corresponding author on reasonable request.

Authors' contributions

The study was conceived and designed by JY. XM, XG and XC conducted the experiments and acquired the data. XM interpreted the results and wrote the first draft of the manuscript. JY made revisions to the final manuscript. All authors read and approved the final manuscript.

Ethics approval and consent to participate

All protocols of the present study were subject to approval by the Ethics Committee of The First Hospital of Jilin University. Written consents were obtained from all participants before surgery.

Patient consent for publication

Not applicable.

Competing interests

The authors declare that they have no competing interests.

References

1. Finnerty CC, Jeschke MG, Branski LK, Barret JP, Dziewulski P and Herndon DN: Hypertrophic scarring: The greatest unmet challenge after burn injury. *Lancet* 388: 1427-1436, 2016.
2. Bombaro KM, Engrav LH, Carrougher GJ, Wiechman SA, Faucher L, Costa BA, Heimbach DM, Rivara FP and Honari S: What is the prevalence of hypertrophic scarring following burns? *Burns* 29: 299-302, 2003.

3. Amini-Nik S, Yousuf Y and Jeschke MG: Scar management in burn injuries using drug delivery and molecular signaling: Current treatments and future directions. *Adv Drug Deliv Rev* 123: 135-154, 2018.
4. Wang H, Pieper J, Peters F, van Blitterswijk CA and Lamme EN: Synthetic scaffold morphology controls human dermal connective tissue formation. *J Biomed Mater Res A* 74: 523-532, 2005.
5. Cutroneo KR: TGF-beta-induced fibrosis and SMAD signaling: Oligo decoys as natural therapeutics for inhibition of tissue fibrosis and scarring. *Wound Repair Regen* 15 (Suppl 1): S54-S60, 2007.
6. Ashcroft GS and Roberts AB: Loss of Smad3 modulates wound healing. *Cytokine Growth Factor Rev* 11: 125-131, 2000.
7. Roberts AB, Russo A, Felici A and Flanders KC: Smad3: A key player in pathogenetic mechanisms dependent on TGF-beta. *Ann N Y Acad Sci* 995: 1-10, 2003.
8. Brunt KR, Weisel RD and Li RK: Stem cells and regenerative medicine-future perspectives. *Can J Physiol Pharmacol* 90: 327-335, 2012.
9. Li Q, Zhang C and Fu X: Will stem cells bring hope to pathological skin scar treatment? *Cytotherapy* 18: 943-956, 2016.
10. Kim KH, Blasco-Morente G, Cuende N and Arias-Santiago S: Mesenchymal stromal cells: Properties and role in management of cutaneous diseases. *J Eur Acad Dermatol Venereol* 31: 414-423, 2017.
11. Yun IS, Jeon YR, Lee WJ, Lee JW, Rah DK, Tark KC and Lew DH: Effect of human adipose derived stem cells on scar formation and remodeling in a pig model: A pilot study. *Dermatol Surg* 38: 1678-1688, 2012.
12. Lam MT, Nauta A, Meyer NP, Wu JC and Longaker MT: Effective delivery of stem cells using an extracellular matrix patch results in increased cell survival and proliferation and reduced scarring in skin wound healing. *Tissue Eng Part A* 19: 738-747, 2013.
13. Hu L, Wang J, Zhou X, Xiong Z, Zhao J, Yu R, Huang F, Zhang H and Chen L: Exosomes derived from human adipose mesenchymal stem cells accelerates cutaneous wound healing via optimizing the characteristics of fibroblasts. *Sci Rep* 6: 32993, 2016.
14. Ding DC, Chang YH, Shyu WC and Lin SZ: Human umbilical cord mesenchymal stem cells: A new era for stem cell therapy. *Cell Transplant* 24: 339-347, 2015.
15. El Omar R, Beroud J, Stoltz JF, Menu P, Velot E and Decot V: Umbilical cord mesenchymal stem cells: The new gold standard for mesenchymal stem cell-based therapies? *Tissue Eng Part B Rev* 20: 523-544, 2014.
16. Dabrowski FA, Burdzinska A, Kulesza A, Sladowska A, Zolocińska A, Gala K, Paczek L and Wielgos M: Comparison of the paracrine activity of mesenchymal stem cells derived from human umbilical cord, amniotic membrane and adipose tissue. *J Obstet Gynaecol Res* 43: 1758-1768, 2017.
17. Xie C, Shi K, Zhang X, Zhao J and Yu J: MiR-1908 promotes scar formation post-burn wound healing by suppressing Ski-mediated inflammation and fibroblast proliferation. *Cell Tissue Res* 366: 371-380, 2016.
18. Livak KJ and Schmittgen TD: Analysis of relative gene expression data using real-time quantitative PCR and the 2(-Delta Delta C(T)) method. *Methods* 25: 402-408, 2001.
19. Brusselaers N, Monstrey S, Vogelaers D, Hoste E and Blot S: Severe burn injury in Europe: A systematic review of the incidence, etiology, morbidity, and mortality. *Crit Care* 14: R188, 2010.
20. Friedstat JS and Hultman CS: Hypertrophic burn scar management: What does the evidence show? A systematic review of randomized controlled trials. *Ann Plast Surg* 72: S198-S201, 2014.
21. Lee DE, Ayoub N and Agrawal DK: Mesenchymal stem cells and cutaneous wound healing: Novel methods to increase cell delivery and therapeutic efficacy. *Stem Cell Res Ther* 7: 37, 2016.
22. Jackson WM, Nesti LJ and Tuan RS: Mesenchymal stem cell therapy for attenuation of scar formation during wound healing. *Stem Cell Res Ther* 3: 20, 2012.
23. Liu S, Jiang L, Li H, Shi H, Luo H, Zhang Y, Yu C and Jin Y: Mesenchymal stem cells prevent hypertrophic scar formation via inflammatory regulation when undergoing apoptosis. *J Invest Dermatol* 134: 2648-2657, 2014.
24. Domergue S, Bony C, Maumus M, Toupet K, Frouin E, Rigau V, Vozenin MC, Magalon G, Jorgensen C and Noël D: Comparison between stromal vascular fraction and adipose mesenchymal stem cells in remodeling hypertrophic scars. *PLoS One* 11: e0156161, 2016.
25. Ding J, Ma Z, Shankowsky HA, Medina A and Tredget EE: Deep dermal fibroblast profibrotic characteristics are enhanced by bone marrow-derived mesenchymal stem cells. *Wound Repair Regen* 21: 448-455, 2013.
26. Weiss DJ: Stem cells and cell therapies for cystic fibrosis and other lung diseases. *Pulm Pharmacol Ther* 21: 588-594, 2008.
27. Tsai PC, Fu TW, Chen YM, Ko TL, Chen TH, Shih YH, Hung SC and Fu YS: The therapeutic potential of human umbilical mesenchymal stem cells from Wharton's jelly in the treatment of rat liver fibrosis. *Liver Transpl* 15: 484-495, 2009.
28. Alatab S, Najafi I, Atlasi R, Pourmand G, Tabatabaei-Malazy O and Ahmadbeigi N: A systematic review of preclinical studies on therapeutic potential of stem cells or stem cells products in peritoneal fibrosis. *Minerva Urol Nefrol* 70: 162-178, 2018.
29. Balasubramanian S, Venugopal P, Sundarraj S, Zakaria Z, Majumdar AS and Ta M: Comparison of chemokine and receptor gene expression between Wharton's jelly and bone marrow-derived mesenchymal stromal cells. *Cytotherapy* 14: 26-33, 2012.
30. Fang S, Xu C, Zhang Y, Xue C, Yang C, Bi H, Qian X, Wu M, Ji K, Zhao Y, *et al*: Umbilical cord-derived mesenchymal stem cell-derived exosomal MicroRNAs suppress myofibroblast differentiation by inhibiting the transforming growth factor-beta/SMAD2 pathway during wound healing. *Stem Cells Transl Med* 5: 1425-1439, 2016.
31. Skalnikova H, Motlik J, Gadher SJ and Kovarova H: Mapping of the secretome of primary isolates of mammalian cells, stem cells and derived cell lines. *Proteomics* 11: 691-708, 2011.
32. Yu B, Zhang X and Li X: Exosomes derived from mesenchymal stem cells. *Int J Mol Sci* 15: 4142-4157, 2014.
33. Kusuma GD, Carthew J, Lim R and Frith JE: Effect of the micro-environment on mesenchymal stem cell paracrine signaling: Opportunities to engineer the therapeutic effect. *Stem Cells Dev* 26: 617-631, 2017.
34. Paschos NK, Brown WE, Eswaramoorthy R, Hu JC and Athanasiou KA: Advances in tissue engineering through stem cell-based co-culture. *J Tissue Eng Regen Med* 9: 488-503, 2015.
35. Goers L, Freemont P and Polizzi KM: Co-culture systems and technologies: Taking synthetic biology to the next level. *J R Soc Interface* 11: pii: 20140065, 2014.
36. Wrzesinski K and Fey SJ: From 2D to 3D-a new dimension for modelling the effect of natural products on human tissue. *Curr Pharm Des* 21: 5605-5616, 2015.



This work is licensed under a Creative Commons Attribution-NonCommercial-NoDerivatives 4.0 International (CC BY-NC-ND 4.0) License.